CHAPTER 11

The plume mode

Mantle plumes are buoyant mantle upwellings that are inferred to exist under some volcanic centres. In Chapter 8 I stated the basic idea that convection is driven by thermal boundary layers that become unstable, detach from the boundary and thereby drive flow in the interior of a fluid layer. In Chapter 10 we looked at plates as a thermal boundary layer of the convecting mantle, driving a distinctive form of convection in the mantle that I called the *plate mode* of mantle convection.

Here we look at the evidence that there is a mode of mantle convection driven by a lower, hot thermal boundary layer, at the expected form of such a mode, and at the consistency of the evidence with that expectation. Since it will become clear that the form and dynamics of such upwellings, or plumes, are quite different from the downwellings of lithosphere driving the plate mode, I will call the plumes and the flow they drive the *plume mode* of mantle convection.

11.1 Volcanic hotspots and hotspot swells

In Chapter 3 I described Wilson's observation that there are, scattered about the earth's surface, about 40 isolated volcanic centres that do not seem to be associated with plates and that seem to remain fixed relative to each other as plates move around (Figure 11.1). Their fixity (or at least their slow motion relative to plate velocities) is inferred from the existence of 'hotspot tracks', that is of chains of volcanoes that are progressively older the further they are from the active volcanic centre. Wilson was building on the inferences of Darwin and Dana that a number of the island chains in the Pacific seem to age progressively along the chain.

The classic example is the Hawaiian volcanic chain of islands and seamounts, evident in the topography shown in Figure 11.2.

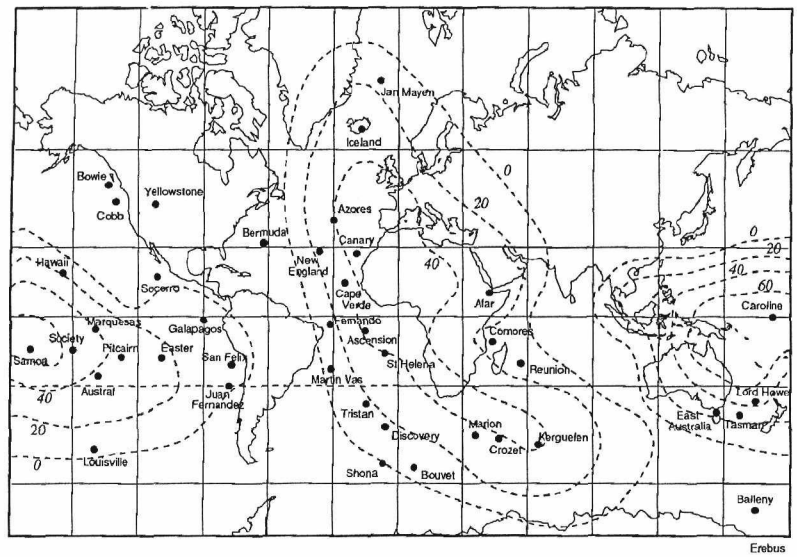

Figure 11.1. Locations of volcanic hotspots (dots). Residual geoid contours (in m) are superimposed (from Crough and Jurdy [1]). The residual geoid may reflect mainly signal from the lower mantle. Hotspots correlate with residual geoid highs but not with the present plate boundaries. From Duncan and Richards [2]. Copyright by the American Geophysical Union.

The south-eastern extremity of this chain, the island of Hawaii, is volcanically active, and the islands and seamounts to the north-west are progressively older. Wilson [3] hypothesised that the source of the eruptions was a 'mantle hotspot' located in a region of the mantle where convective velocities are small, such as the middle of a convection 'cell'. Morgan [4, 5] proposed instead that the source of the eruptions is a mantle plume, that is a column of hot, buoyant mantle rising from the core–mantle boundary.

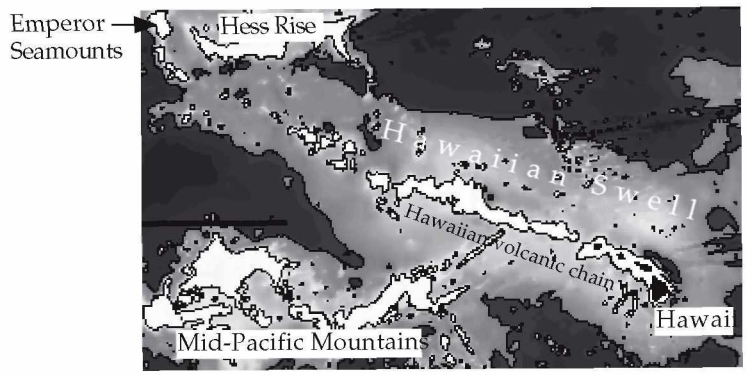

Figure 11.2. Topography of the sea floor near the Hawaiian Islands, showing the volcanic chain of islands and seamounts and the broad swell surrounding them. The contours are at depths of 3800 m and 5400 m.

Wilson's hypothesis had the disadvantages that the existence of the mantle hotspot was *ad hoc*, with no obvious reason for being there, and that it was not clear how a finite volume of warmer mantle could provide a steady supply of volcanism for tens of millions of years. Morgan's hypothesis at least implied a plausible physical source and the potential for longevity. Morgan's hypothesis immediately became the preferred one. Because of this, I proposed, in Chapter 3, dropping the concept of an internal mantle hotspot, and using the term 'volcanic hotspot' for the surface expression of the mantle phenomenon.

The number of volcanic hotspots has been variously estimated between about 40 [1, 6] and over 100 [7], but it is debatable whether many of the latter might be associated with individual mantle plumes. Figure 11.1 shows 40 hotspot locations selected by Duncan and Richards [2]. Contours of the hydrostatic geoid (i.e. relative to the shape of a rotating hydrostatic earth) are included. The suggestion is that hotspots correlate with highs in the geoid, which plausibly are due to structure in the lower mantle (Chapter 10), and specifically to regions of the deep mantle that are warmer because there has been no subduction into them in the past 200 Ma or so [8]. On the other hand, it is striking that hotspots show little correlation with the present configuration of plate boundaries.

As well as the narrow topography of the Hawaiian volcanic chain, there is evident in Figure 11.2 a broad swell in the sea floor surrounding the chain. This swell is up to about 1 km high and about 1000 km wide. Such a swell might be due to thickened oceanic crust, to a local imbalance of isostasy maintained by the strength of the lithosphere, or to buoyant material raising the lithosphere. Seismic reflection profiles show that the oceanic crust is not significantly thicker than normal [9]. Nor can such a broad swell be held up by the flexural strength of the lithosphere. The colder parts of the lithosphere behave elastically even on geological time scales, as long as their yield stress is not exceeded. For lithosphere of the age of that near Hawaii, about 90 Ma, the effective elastic thickness of the lithosphere is about 30 km thick, and it has a flexural wavelength of about 500 km [10]. However the wavelength of the swell is about 2000 km. If the swell were held out of isostatic balance by the lithosphere, the stresses would exceed the plausible yield stress of the lithosphere.

The straightforward conclusion is that the Hawaiian swell is held up by buoyant material under the lithosphere. In conjunction with the existence of the isolated volcanic centre, it is then a straightforward inference that there is a narrow column of hot mantle rising under Hawaii. Both the unusual volcanism and the

supply of buoyancy to the base of the lithosphere would be explained if the column had a higher temperature than normal mantle. The volcanism occurs in a small, isolated locality far from plate boundaries, in contrast, for example, to the curvilinear volcanic island arcs near subduction zones. The isolation implies that the buoyant material is in the form of a column rather than a sheet. Since the active volcanism is confined to within an area of the order of 100 km across, it is reasonable to infer that the column diametre is of the same order. The fact that the Hawaiian hotspot track extends, through the bend into the Emperor seamounts, to ages of at least 90 Ma indicates that the mantle source is long-lived, and not due to an isolated heterogeneity within the mantle. Morgan called such a hot, narrow column a *mantle plume*.

11.2 Heat transported by plumes

Swells like that in Figure 11.2 are evident around many of the identified volcanic hotspots. Other conspicuous examples are at Iceland, which straddles the Mid-Atlantic Ridge, and at Cape Verde, off the west coast of Africa (Figure 4.3). The latter is 2 km high and even broader than the Hawaiian swell, presumably because the African plate is nearly stationary relative to the hotspot [2].

The swells can be used to estimate the rate of flow of buoyancy in the plumes. Buoyancy, as we saw in Chapter 8, is the gravitational force due to the density deficit of the buoyant material. If the plume is envisaged as a vertical cylinder with radius r and if the plume material flows upward with an average velocity u (as in Figure 7.7), then the buoyancy flow rate is

$$b = g\Delta\rho \cdot \pi r^2 u \tag{11.2.1}$$

where $\Delta\rho = (\rho_p - \rho_m)$ is the density difference between the plume and the surrounding mantle.

The way buoyancy flow rate can be inferred from hotspot swells is clearest in the case of Hawaii. The Hawaiian situation is sketched in Figure 11.3, which shows a map view and two cross-sections. As the Pacific plate moves over the rising plume column it is lifted by the plume buoyancy. There will be a close isostatic balance between the weight of the excess topography created by this uplift and the buoyancy of the plume material under the plate, as we discussed in Section 8.8. Since the plate is moving over the plume, the parts of the plate that are already elevated are being carried away from the plume. In order for the swell to persist, new

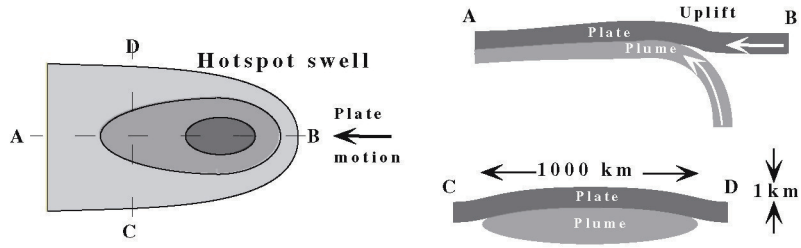

Figure 11.3. Sketch of a hotspot swell like that of Hawaii (Figure 11.2) in map view (left) and two cross-sections, showing the relationship of the swell to the plume that is inferred to be below the lithosphere. The swell is inferred to be raised by the buoyancy of the plume material. This allows the rate of flow of buoyancy and heat in the plume to be estimated.

parts of the plate have to be continuously raised as they arrive near the plume. This requires the arrival of new buoyant plume material under the plate (cross-section AB). Thus the rate at which new swell topography is generated will be a measure of the rate at which buoyant plume material arrives under the lithosphere.

The addition to swell topography each year is equivalent to elevating by a height $h = 1\,\text{km}$ a strip of sea floor with a 'width' $w = 1000\,\text{km}$ (the width of the swell) and a 'length' $v\delta t = 100\,\text{mm}$ (the distance travelled by the Pacific plate over the plume in one year at velocity $v = 100\,\text{mm/a}$). Both the sea floor and the Moho are raised, and sea water is displaced, so the effective difference in density is that between the mantle (ρ_m) and sea water (ρ_w). The rate of addition to the weight (negative buoyancy) of the new swell is then

$$W = g(\rho_\text{m} - \rho_\text{w})wvh = b \tag{11.2.2}$$

By the argument just given, the buoyancy flow rate b in the plume is equal to W. Using the values quoted above yields $b = 7 \times 10^4\,\text{N/s}$ for Hawaii.

If the plume buoyancy is thermal, it can be related to the rate of heat transport by the plume, since both depend on the excess temperature, $\Delta T = T_\text{p} - T_\text{m}$, of the plume. Thus the difference between the plume density, ρ_p, and the mantle density is

$$\rho_\text{p} - \rho_\text{m} = \rho_\text{m}\alpha\Delta T \tag{11.2.3}$$

while the heat flow rate is (see Section 7.7)

$$Q = \pi r^2 u \rho_\text{m} C_P \Delta T \tag{11.2.4}$$

Taking the ratio of Q and b and using Equation (11.2.3) then yields

$$Q = C_P b/g\alpha \tag{11.2.5}$$

Note particularly that this relationship does not depend on the excess temperature of the plume. In fact this is the same relationship as we derived in Section 10.4.4 between the buoyancy and heat flow rates of plates (Equation (10.4.4)). Thus this is another specific and quantitative example of the general relationship between convection and topography that we discussed in Section 8.8.

With $C_P = 1000\,\text{J/kg}\,^\circ\text{C}$ and $\alpha = 3 \times 10^{-5}/^\circ\text{C}$ this yields roughly $Q = 2 \times 10^{11}\,\text{W}$, which is about 0.5% of the global heat flow. The total rate of heat transport by all known plumes has been estimated very roughly by Davies [11], and more carefully by Sleep [12], with similar results. Although there are 40 or more identified hotspots, all of them are weaker than Hawaii and many of them are substantially weaker. The total heat flow rate of plumes is about $2.3 \times 10^{12}\,\text{W}$ (2.3 TW), which is about 6% of the global heat flow (41 TW, Table 10.1).

This value is comparable to estimates of the heat flow out of the core. Stacey [13] estimated this from the thermal conductivity of the core and its adiabatic temperature gradient, obtaining 3.7 TW for the heat that would be conducted down this gradient. Convective heat transport in the core would add to this, but compositional convection, due to continuing solidification of the inner core, might subtract from it. Another estimate can be made from thermal history calculations (Chapter 14), in which the core cools by several hundred degrees through earth history. Taking the present cooling rate to be about $70\,^\circ\text{C/Ga}$, the core mass to be $1.94 \times 10^{20}\,\text{kg}$ and the specific heat to be $500\,\text{J/kg}\,^\circ\text{C}$ yields a rate of heat loss of about 2.3 TW.

These estimates carry substantial uncertainty. As well, the estimate of plume heat flow rate should include the heat carried by plume heads (Sections 11.4, 11.5). Hill *et al.* [14] used the frequency of flood basalt eruptions in the geological record of the past 250 Ma to estimate that plume heads carry approximately 50% of the heat carried by plume tails. Thus the total heat flow rate in plumes would be approximately 3.5 TW, less than 10% of the global heat flow rate.

The approximate correspondence of the estimate of the heat transported by plumes with the rate of heat loss from the core supports Morgan's proposal that plumes come from a thermal boundary layer at the base of the mantle. According to our general discussion of convection in Chapter 8, a bottom thermal boundary

layer is formed when heat enters through the bottom boundary of a fluid layer.

Stacey and Loper [15] were apparently the first to appreciate that this implies that plumes are cooling the core, in the sense that they are the agent by which heat from the core is mixed into the mantle. In this interpretation, the role of plumes is primarily to transfer heat from the core *through* the mantle, but not *out of* the mantle. Plumes bring heat to the base of the lithosphere, which is mostly quite thick and conducts heat only very slowly to the surface. For example, no excess heat flux has been consistently detected over the Hawaiian swell [16]. While in some cases, like Iceland, the lithosphere is thin and a substantial part of the excess plume heat may be lost to the surface, more commonly much of the plume heat would remain in the mantle, presumably to be mixed into the mantle after the overlying lithosphere subducts.

11.3 Volume flow rates and eruption rates of plumes

It was stressed above that the buoyancy flow rate of a plume can be estimated from the swell size without knowing the plume temperature. However, if we do have an estimate of plume temperature it is then possible to estimate the volumetric flow rate of the plume. It is instructive to compare this with the rate of volcanic eruption.

From the petrology of erupted lavas, plumes are estimated to have a peak temperature of 250–300 °C above that of normal mantle [17]. The volumetric flow rate up the plume is $\Phi_p = \pi r^2 u$, where u is the average velocity in the conduit and r is its radius. From Equations (11.2.1) and (11.2.3), this is related to the buoyancy flow rate, b, by

$$\Phi_p = b/g\rho_m\alpha\Delta T \tag{11.3.1}$$

b was also related to the rate at which the swell volume is created, $\Phi_s = wvh$, through the weight of topography, W, in Equation (11.2.2):

$$\Phi_s = wvh = W/g(\rho_m - \rho_w) = b/g(\rho_m - \rho_w) \tag{11.3.2}$$

so the plume volumetric flow rate is related to the swell volumetric rate of creation through

$$\Phi_p = \Phi_s(\rho_m - \rho_w)/\rho_m\alpha\Delta T \tag{11.3.3}$$

For example, for Hawaii $\Phi_s = 0.1\,km^3/a$. If $\rho_m = 3300\,kg/m^3$, $\rho_w = 1000\,kg/m^3$, $\alpha = 3 \times 10^{-5}/°C$ and $\Delta T = 300\,°C$, then $(\rho_m - \rho_w)/\rho_m \alpha \Delta T = 75$. In other words the plume volumetric flow rate is about 75 times the rate of uplift of the swell. Thus for Hawaii $\Phi_p = 7.5\,km^3/a$.

The Hawaiian eruption rate, that is the rate at which the volcanic chain has been constructed, has been about $\Phi_e = 0.03\,km^3/a$ over the past 25 Ma [18, 19]. It is immediately evident that this is very much less than the plume volumetric flow rate. It implies that only about 0.4% of the volume of the plume material is erupted as magma at the surface. Even if there is substantially more magma emplaced below the surface, such as at the base of the crust under Hawaii [9, 20], the average melt fraction of the plume is unlikely to be much more than 1%.

Since the magmas show evidence of being derived from perhaps 5–10% partial melting of the source [17, 21], this presumably means that about 80–90% of the plume material does not melt at all, and the remainder undergoes about 5–10% partial melt. This result is important for the geochemical interpretation of plume-derived magmas and it is also useful for evaluating an alternative hypothesis for the existence of hotspot swells (Section 11.6.3).

11.4 The dynamics and form of mantle plumes

Having looked at the observational evidence for the existence of mantle plumes, and having derived some important measures of them, we now turn to the fluid dynamics of buoyant upwellings. Our understanding of the physics of such upwellings is quite well-developed, and there are some inferences and predictions that can be made with considerable confidence. This means that the hypothesis of mantle plumes can potentially be subjected to a number of quantitative observational tests.

This understanding of plume dynamics has arisen from some mathematical results, some long-standing and some more recent, and from some elegant laboratory experiments supplemented by physical scaling analyses and some numerical modelling. Plume dynamics is more tractable than plate dynamics largely because plumes are entirely fluid.

11.4.1 Experimental forms

The buoyant upwellings from a hot thermal boundary layer might have the form of sheets or columns. The downwellings driven by sinking plates clearly have the form of sheets, at least in the upper

part of the mantle, since plates are stiff sheets at the surface and subduct along continuous curvilinear trenches. The stiffness of the plate would be expected to preserve this form to some depth, and recent results of seismic tomography seem to confirm this expectation (Chapter 5).

In contrast, Whitehead and Luther [22] showed experimentally and mathematically that upwellings from a buoyant fluid layer preferentially form columns rather than sheets. In experiments starting with a thin uniform fluid layer underlying a thick layer of a more dense fluid, the less dense fluid formed upwellings that started as isolated domes, rather than as sheets. Whitehead and Luther supplemented this laboratory demonstration with a mathematical analysis of second-order perturbation theory that showed that the rate of growth of a columnar upwelling is greater than the rate of growth of a sheet upwelling. This is an extension of the Rayleigh–Taylor instability that we encountered in Section 8.4.

Whitehead and Luther's experiments also demonstrated that the viscosity of an upwelling relative to the viscosity of the fluid it rises through has a strong influence on the form of the upwelling. This is illustrated in Figure 11.4, which shows buoyant upwellings

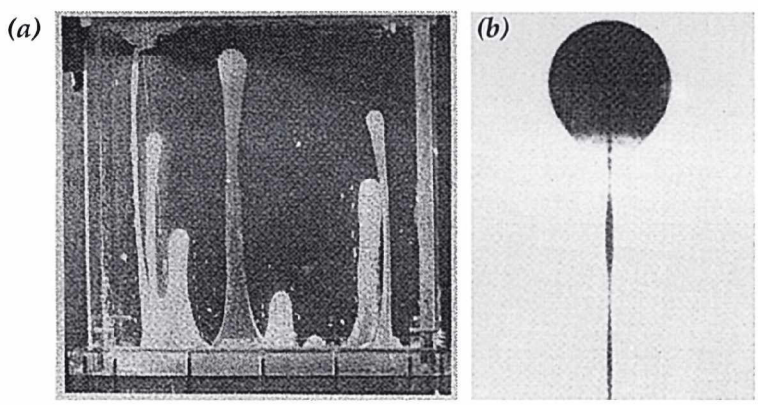

Figure 11.4. Photographs from laboratory experiments showing the effect of viscosity on the forms of buoyant upwellings. (a) The buoyant fluid is more viscous than the fluid it rises through, and the upwellings have fairly uniform diameter. In this case the buoyant fluid began as a thin uniform layer at the base of the tank. From Whitehead and Luther [22]. Copyright by the American Geophysical Union. (b) The buoyant fluid is less viscous than the fluid it rises through, and the upwelling has the form of a large spherical head and a thin columnar tail. In this case the buoyant fluid was injected through the base of the tank, and dyed to distinguish it. From Richards, Duncan and Courtillot [23]. Copyright American Association for the Advancement of Science. Reprinted with permission.

rising from the base of a tank. If the buoyant fluid is much more viscous than the ambient fluid (Figure 11.4a), the diameter of the buoyant columns is fairly uniform over its height. If the buoyant fluid is much less viscous (Figure 11.4b), then the column has a large, nearly spherical head at the top with a very thin conduit or tail connecting it to source. The reason for these different forms can be understood fairly simply, and this will be addressed in the next section.

Each of the experiments shown in Figure 11.4 involved two different fluids with different densities and viscosities. However, in the mantle we expect that the material ascending in a plume is the same material as normal mantle, but hotter. The higher temperature would make the plume less dense, and also lower its viscosity (Section 6.10.2). We might expect therefore that a mantle upwelling from a hot thermal boundary layer would form a plume, and that the plume would have a head-and-tail structure, as in Figure 11.4b. This is confirmed by the experiment illustrated in Figure 11.5a which shows a plume formed by heating a fluid whose viscosity is a strong function of temperature. The viscosity of the plume fluid is about 0.3% of the viscosity of the surrounding fluid, and the plume has a pronounced head-and-tail structure.

A striking new feature in Figure 11.5a is that the injected fluid forms a spiral inside the plume head. This is caused by thermal entrainment of surrounding, clear fluid into the head. As the head rises, heat diffuses out of it into the surrounding, cooler fluid, forming a thermal boundary layer around the head. Because this fluid is heated, it becomes buoyant, and so it tends to rise with the head. The spiral structure forms because there is a circulation within the plume head, with an upflow in the centre, where hot new fluid is arriving from the conduit, and a relative downflow around the equator, where the rise of the plume is resisted by the surrounding fluid. The fluid from the thermal boundary layer around the head is entrained into this internal circulation, flowing up next to the central conduit. This process is quantified in Section 11.4.3.

Thermal entrainment is not so important if the plume fluid is cold. Figure 11.5b shows a column of cold, dense, more viscous fluid descending into the same kind of fluid. The subdued head-and-tail structure is due to some of the surrounding fluid cooling and descending with the plume, but the resistance to the head from the surrounding lower-viscosity fluid is not sufficient to generate a significant internal circulation in the head, so there is no entrainment into it.

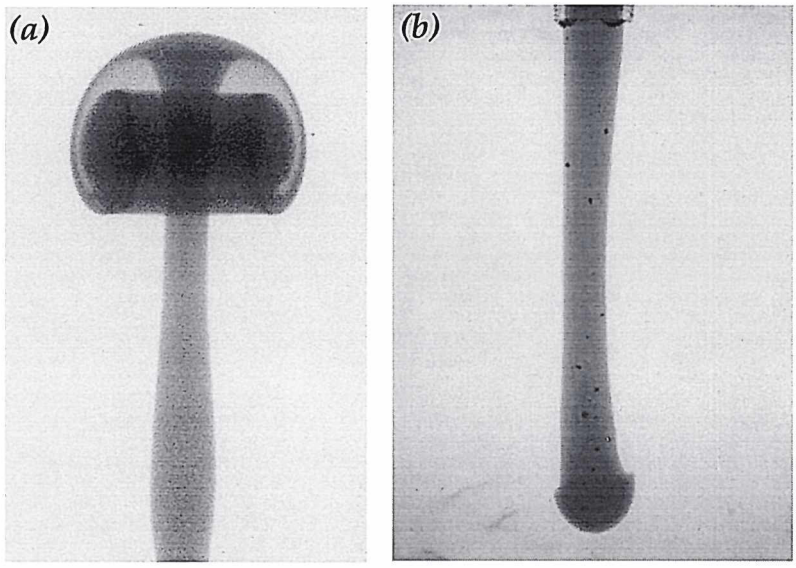

Figure 11.5. Thermal plumes in laboratory experiments, formed by injecting hot or cold dyed fluid into otherwise identical fluid. The fluid has a strong temperature dependence of viscosity. (a) The buoyant fluid is hot, and the plume viscosity is about 1/300 times that of the surrounding fluid. A spiral structure forms in the head due to thermal entrainment of ambient fluid. From Griffiths and Campbell [24]. (b) The injected fluid is cooler and hence denser and more viscous than the ambient fluid. There is little entrainment of cooled surrounding fluid, and only a very small head forms. From Campbell and Griffiths [25]. Copyright by Elsevier Science. Reprinted with permission.

Returning to the hot, low-viscosity plume of Figure 11.5a, similar structures are formed if a plume grows from a hot thermal boundary layer and the fluid viscosity is a strong function of temperature. Results of a numerical experiment scaled approximately to the mantle are shown in Figure 11.6. The panels are sections through an axisymmetric model showing the growth of a plume from an initial perturbation in the boundary layer. A line of passive tracers delineates the fluid initially within the hot boundary layer. The tracers reveal that the boundary layer fluid forms a spiral in the head due to thermal entrainment, as in Figure 11.5a. This numerical model also reveals the thermal structure within the plume. The hottest parts of the plume are the tail and the top of the head, where the tail material spreads out. Most of the head is cooler, and there are substantial thermal gradients within it. Temperatures within the head are intermediate between the plume tail temperature and the surrounding fluid.

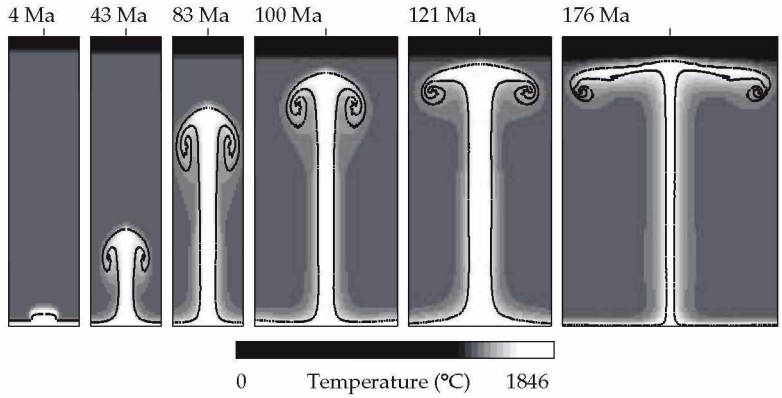

Figure 11.6. Sequence from a numerical model in which a plume grows from a thermal boundary layer. The model is axisymmetric and scaled approximately to the mantle. Viscosity is a strong function of temperature, and the ambient viscosity is 10^{22} Pa s. The bottom boundary temperature is 430 °C above the interior temperature, and the fluid viscosity there is about 1% of that of the interior fluid. A line of passive tracers delineates fluid initially within the thermal boundary layer.

11.4.2 Heads and tails

Here we look at why low-viscosity plumes form a head-and-tail structure. In the case in which the plume has a higher viscosity than the surroundings, the rise of the plume is limited mainly by the viscous resistance within the plume itself and within the boundary layer that feeds it. This means that the fluid in the plume does not rise faster than the top or head, and so it does not accumulate into a large head. The moderate variation of thickness with height is explained by the stretching of the column as the top rises faster than the stiff fluid can flow after it.

On the other hand, in the case where the plume has a lower viscosity, the plume fluid can flow readily from the boundary layer into and up the plume, and the main resistance to its rise comes from the surrounding more viscous fluid, which must be pushed out of the way. In this situation, the rise of the top of the plume is analogous to the rise of a buoyant sphere, and is regulated by the same balance of buoyancy and viscous resistance. In Chapter 6 we derived the Stokes formula for the velocity at which a buoyant sphere rises (Equation (6.8.3)). In fact you can see that the heads of the plumes in Figures 11.4b and 11.5a closely approximate a sphere. The role of this sphere is to force a path through the more viscous surroundings. Its rate of rise is initially slow, but it grows by the addition of plume fluid flowing out of the boundary layer. Once the head is large enough to force a path, the low-

viscosity plume fluid can readily follow, requiring only a narrow conduit to flow through, its rate of flow being regulated by the rate at which it can flow out of the thin boundary layer. This is why the conduit trailing the head can have a much smaller radius.

The way the head-and-tail structure of plumes depends on the viscosity contrast between the plume and its surroundings is illustrated further in Figure 11.7. This shows three numerical models of plumes with different ratios of plume viscosity to surrounding viscosity: respectively 1, 1/30 and 1/200. The size of the head is similar in each case, but the conduit is thinner for the lower viscosities, reflecting the fact that the lower viscosity material requires only a thin conduit for a similar rate of flow.

11.4.3 Thermal entrainment into plumes

We will now consider the thermal structure of plumes in more detail. As the hot fluid in the conduit reaches the top of the head, it spreads radially out and around the periphery of the sphere, becoming very thin because of the greater radius of the head (Figures 11.6, 11.7). Because it is thinned, its heat diffuses out much more quickly (remember, from Chapter 7, that a diffu-

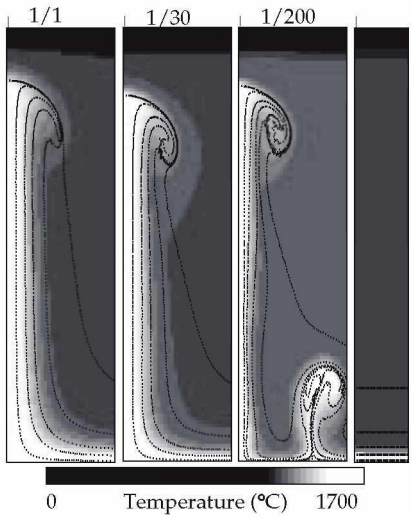

Figure 11.7. Plumes from three numerical models with different ratios of minimum plume viscosity to ambient viscosity, respectively 1, 1/30 and 1/200, showing how the tail is thinner for lower-viscosity plumes. The models are axisymmetric about the left-hand side of each panel. Several lines of tracers in this model mark fluid from different levels in the box. The initial configuration is shown in the right-hand panel. A secondary instability has developed in the right-hand model.

sion time scale is proportional to the square of the length scale involved). This heat goes partly outwards, to form the thermal boundary layer around the head, and partly inwards, to further heat the entrained material wrapping under it. As a result, the head has a temperature intermediate between that of the conduit and the surroundings. The spiral structure of the plume fluid, which is revealed by the dye in Figure 11.5a and by the tracers in Figures 11.6 and 11.7, is not evident in the thermal structure, because it is smoothed out by thermal diffusion. There are still thermal gradients in the head, but they are subdued relative to the temperature difference between the conduit and the surroundings.

The additional lines of tracers in Figure 11.7 reveal that most of the material entrained into the head comes from the lowest 10–20% of the fluid layer. Since these numerical experiments are scaled approximately to the mantle, this conclusion will apply also to plumes in the mantle. This is important for the interpretation of the geochemistry of flood basalts (Section 11.5).

We can quantify the rate of entrainment into a plume head using our understanding of thermal diffusion (Section 7.2) and of rising buoyant spheres (Section 6.8), following the approach used by Griffiths and Campbell [24]. The situation is sketched in Figure 11.8. We take the approach of using approximations that are rough, but that scale in the appropriate way. The thickness, δ, of the thermal boundary layer adjacent to the hot plume head will depend on the time the adjacent fluid is in contact with the passing plume head. This time will be of the order of $2R/U$, where the plume head radius is R and its rise velocity is U. Then, from Section 7.2,

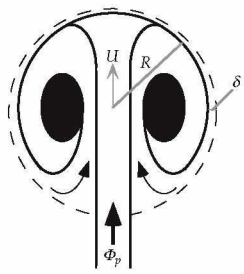

Figure 11.8. Sketch of a thermal boundary layer around a hot plume head. The fluid in the thermal boundary layer is heated by diffusion from the head. It is then buoyant and is entrained into the head. Boundary layer thickness is δ, head radius is R, head rise velocity is U and the volumetric flow rate up the plume tail is Φ_p.

$$\delta = \sqrt{\kappa t} = \sqrt{\frac{2\kappa R}{U}} \tag{11.4.1}$$

where κ is the thermal diffusivity. The horizontal cross-sectional area of the boundary layer near the head's equator is the head circumference times this thickness, $2\pi R\delta$, and the rate at which boundary layer fluid flows through this area is

$$\Phi_e = 2\pi R\delta U \tag{11.4.2}$$

We can assume that this fluid, or a constant fraction of it, becomes entrained into the head, so that Φ_e is an estimate of the volumetric rate of entrainment. The velocity, U, at which the head rises is given by the Stokes formula for a low-viscosity sphere (Section 6.8):

$$U = \frac{g\rho\alpha\Delta T R^2}{3\mu} \tag{11.4.3}$$

where ρ, α and μ are the density, thermal expansion coefficient and viscosity of the fluid respectively and ΔT is the temperature difference between the head and its surroundings.

If we take standard mantle values for these quantities (Appendix 2) with a viscosity appropriate for lower mantle, $\mu = 10^{22}$ Pa s, a temperature difference of 100 °C and a radius of 500 km, this yields a rise velocity of $U = 7 \times 10^{-10}$ m/s = 20 mm/a. The boundary layer thickness is then 40 km and the rate of entrainment is 2.7 km^3/a. This is comparable to the volume flow rate inferred for the Hawaiian plume tail of 7.5 km^3/a, which is the strongest plume tail by about a factor of 3 [11, 12]. The rate of increase of the head radius due to entrainment is

$$\frac{\partial R}{\partial t} = \frac{\Phi_e}{4\pi R^2} \tag{11.4.4}$$

With the values just derived, the rate of increase of radius is 1 mm/a = 1 km/Ma. This compares with a rise velocity of 20 mm/a.

This may suggest that entrainment is not very important, but Griffiths and Campbell integrated Equations (11.4.1–3), taking account of the influx from the tail, Φ_p, and the drop in average temperature as the entrainment proceeds. As cool fluid is entrained, the heat content of the plume is diffused through a larger volume. If the rate of inflow of fluid, Φ_p, is constant, the total heat supplied is proportional to $\Delta T_s \Phi_p (t - t_0) = \Delta T_s \Phi_p \Delta t$, where ΔT_s is the temperature excess of the source and Δt is the duration of the inflow. If the head volume at a later time is V, then conservation of energy requires that

$$\Delta T = \Delta T_s \Phi_p \Delta t / V \tag{11.4.5}$$

Combining Equations (11.4.1–3) with this yields

$$\Phi_e = 2\pi R \left[\frac{\kappa g \rho \alpha \Delta T_s \Phi_p \Delta t}{2\pi\mu} \right]^{1/2} \tag{11.4.6}$$

Then we can write an equation for the radius as a function of time as

$$\frac{\partial R}{\partial t} = \frac{\Phi_p + \Phi_e}{4\pi R^2} \tag{11.4.7}$$

Griffiths and Campbell found that plume head sizes of about 500 km radius at the top of the mantle are predicted rather consistently, independent of the tail flow rate and the temperature difference of the plume fluid source. Some of their results are shown in Figure 11.9. The initial rate of increase of the radius is much greater than it is as the head nears the top of the mantle, which explains the slow rates estimated above. Most of the curves in Figure 11.9 are for a mantle viscosity of 10^{22} Pa s, believed to be appropriate for the deep mantle where most of the head growth occurs. A lower viscosity of 10^{21} might be appropriate for the mantle in the Archean, and a smaller head is then predicted (Figure 11.9a). The plume head in the numerical experiment of Figure 11.6 approaches 1000 km in diameter near the top, consistent with their predictions. Taking the box depth to be 3000 km, the thermal halo in the fourth panel is 1000 km across and the tracers span about 800 km.

Entrainment may also occur into a plume tail. When the tail is vertical, as in Figures 11.6,7,10, this is so small that it is not evident in any obvious way. In fact Loper and Stacey have calculated that a strictly vertical plume tail with a strong viscosity contrast would entrain only a small percentage of additional material. Presumably this is because the travel time of the fluid up the conduit is short enough that diffusive heat loss to the surroundings is small. In the

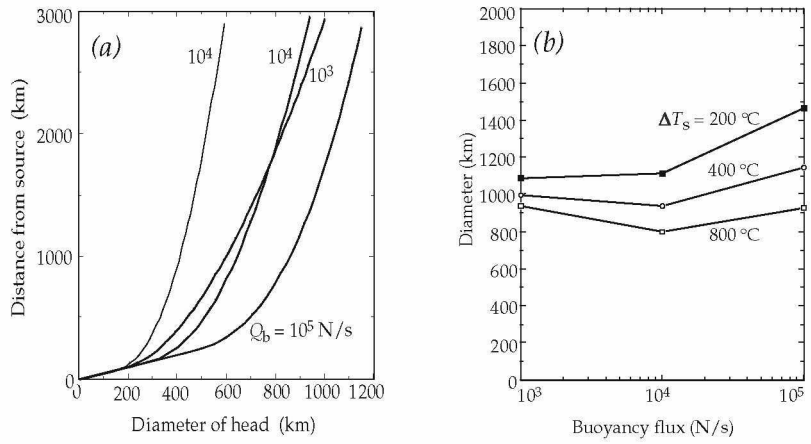

Figure 11.9. (a) Predicted plume head diameter versus height risen in a mantle of viscosity 10^{22} Pa s (heavy) and 10^{21} Pa s (light). Curves are labelled with buoyancy flow rate $Q_b = g\Delta\rho\Phi_p$. (b) Predicted plume head diameter at the top of the mantle for a mantle viscosity of 10^{22} Pa s and a range of buoyancy flow rates in the plume tail and fluid source excess temperatures, ΔT_s. From Griffiths and Campbell [24]. Copyright by Elsevier Science. Reprinted with permission.

numerical experiment depicted in the right-hand panel of Figure 11.7 the temperature in the centre of the conduit varies by only about 3% over most of its height. On the other hand, if the plume tail is inclined to the vertical, as it would be if the surrounding fluid were moving horizontally, then entrainment occurs by the same mechanism as for the plume head, and substantially larger degrees of entrainment may occur. This has been demonstrated experimentally by Richards and Griffiths [26].

11.4.4 Effects of a viscosity step and of phase changes

Figure 11.6 showed a numerical model of a thermal plume in which the viscosity depends on temperature. However, in the mantle the viscosity is also believed to vary substantially with depth, as discussed in Chapters 6 and 10. As well, phase transformations in the mantle transition zone may affect the rise of plumes, as discussed in Section 5.3, and the descent of subducted lithosphere discussed in Chapter 10.

The effects of including depth dependence of viscosity and a phase transformation are illustrated by the sequence from a numerical model shown in Figure 11.10. The viscosity increases with depth in a similar way to the models in Figure 10.12: there is a step by a factor of 20 at 700 km and an exponential increase by a factor of 10. As the plume head rises, its top feels the viscosity reducing and rises faster, stretching the plume head vertically.

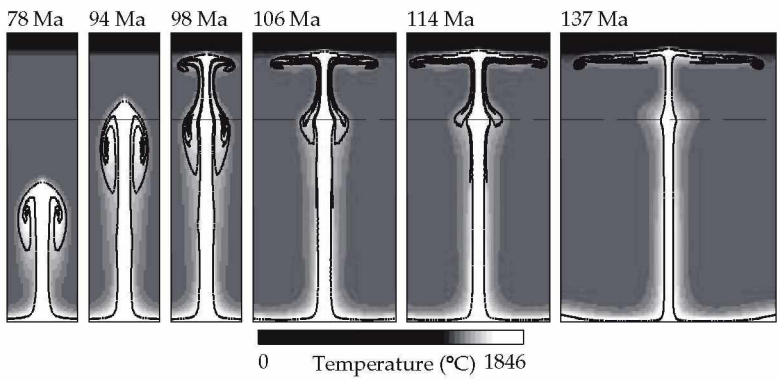

Figure 11.10. Sequence from a numerical plume model including increasing viscosity with depth and a phase transformation. The viscosity steps by a factor of 20 at 700 km depth and has an exponential increase by a factor of 10. The phase transformation at 700 km depth has a Clapeyron slope of −2 MPa/K. The plume slows and thickens through the phase transformation, but then narrows and speeds up in the low-viscosity upper layer.

This becomes pronounced as it enters the low-viscosity upper layer, where its rate of ascent increases and it necks down to a narrower diameter. As it then rises through the upper layer, it begins to form a second entrainment spiral, resulting in some convolution of the original spiral structure. The plume tail also speeds up and becomes narrower as it enters the upper layer (last frame).

This model also includes the effect of a phase transformation at 700 km depth with a moderately negative Clapeyron slope of −2 MPa/K. In this case the effect is not sufficient to block the ascent of the plume, though it does slow its rise in the vicinity of the phase transformation. This is most clearly evident in the last frame, where the plume tail bulges out as it slows, and then narrows again as it passes the phase transformation and enters the low-viscosity upper layer.

Compared with the plume in Figure 11.6, this plume reaches a shallower level. This is because it is much narrower as it rises into the upper mantle, and it does not trap as much mantle between itself and the lithosphere. Also as it spreads it is significantly thinner than in Figure 11.6, because of the lower viscosity below the lithosphere. Because it spreads faster, the high-temperature region is broader. These features are significant for the plume head model of flood basalts (Section 11.5), since they tend to promote greater melting over a broader area than in the model of Figure 11.6.

The effects of phase transformations with more negative Clapeyron slopes are illustrated by the models in Figure 11.11 [27]. As we have just seen in Figure 11.10, if the Clapeyron slope is −2 MPa/K, the plume continues through, and it is virtually unchanged except for a local bulge where its ascent is slowed by the phase transformation. If the Clapeyron slope is −3 MPa/K, then the plume is unable to penetrate. Apparently, if it does not penetrate immediately, then it spreads sufficiently rapidly that it

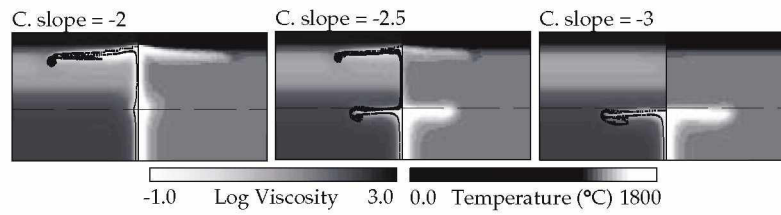

Figure 11.11. Plume models like that in Figure 11.10, but with different Clapeyron slopes (C. slope) of the phase transformation. The viscosity structure is shown on the left of these panels and the temperature on the right. From Davies [27]. Copyright by Elsevier Science. Reprinted with permission.

cannot ever penetrate. If the Clapeyron slope is −2.5 MPa/K, then the main part of the plume head penetrates but the tail is choked off and accumulates below the phase boundary. This would give rise to a tailless head in the upper mantle. (The precise value of the Clapeyron slope at which plume penetration is blocked is dependent on other details of the models, so these models should not be taken as a precise determination, but as a reasonable illustration of the process.)

11.5 Flood basalt eruptions and the plume head model

In Sections 11.1–3 we looked at observations that can be interpreted to relate to plume tails. It was the age-progressive volcanic chains that originally motivated Morgan's plume hypothesis, a model that we now identify more specifically as a plume tail. In 1981, Morgan [6] pointed out that several hotspot tracks emerged from flood basalt provinces. A notable example is the Chagos–Laccadive Ridge running south from the Deccan Traps flood basalt province in western India to Reunion Island in the Indian Ocean (Figures 4.3, 11.12).

Flood basalts are evidence of the largest volcanic eruptions identified in the geological record. They range up to 2000 km across, with accumulated thicknesses of basalt flows up to several kilometres. A map of the main identified flood basalt provinces is shown in Figure 11.12. Total volumes of extrusive eruptions range up to 10 million cubic kilometres, and evidence is accumulating that much of this volume is erupted in less than 1 million years [28]. It has been recognised within the past decade that some oceanic plateaus are oceanic equivalents of continental flood basalts. The largest flood basalt province is the Ontong–Java Plateau, a submarine plateau east of New Guinea.

Morgan [6] proposed that if flood basalts and hotspot tracks are associated, then the head-and-tail structure of a new plume, which had been demonstrated by Whitehead and Luther, would provide an explanation. Figure 11.13 illustrates the concept. The flood basalt eruption would be due to the arrival of the plume head, and the hotspot track would be formed by the tail following the head. If the overlying plate is moving, then the flood basalt and the underlying head remnant would be carried away, and the hotspot track would emerge from the flood basalt province and connect it to the currently active volcanic centre, which would be underlain by the active plume tail.

Not a lot of attention was given to Morgan's proposal until Richards, Duncan and Courtillot [23] revived and advocated the

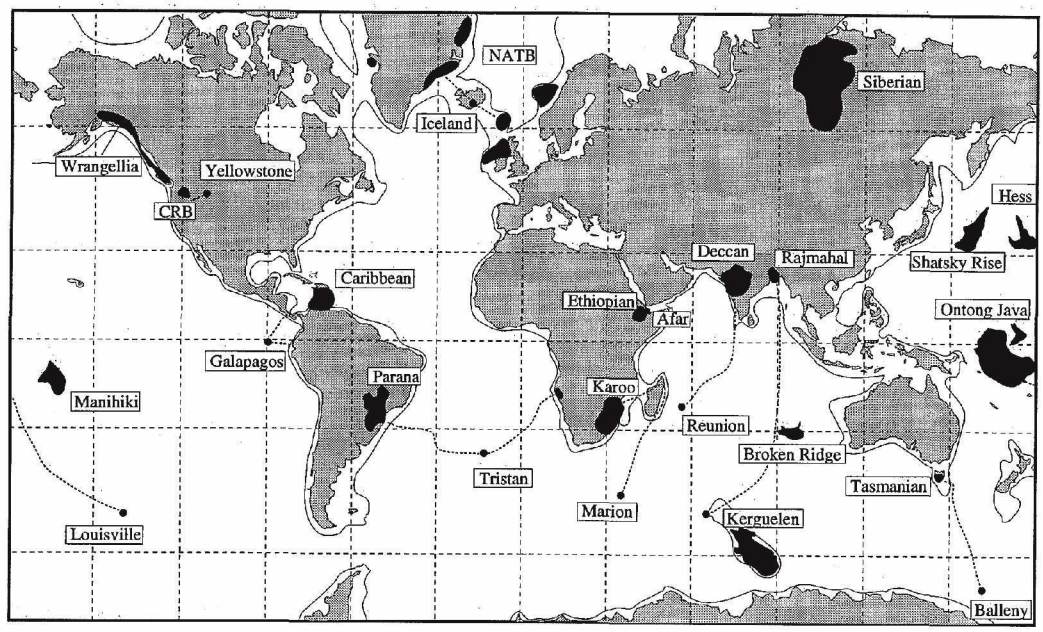

Figure 11.12. Map of continental and oceanic flood basalt provinces. Dotted lines show known or conjectured connections with active volcanic hotspots. After Duncan and Richards [2]. Copyright by the American Geophysical Union.

idea. Subsequently Griffiths and Campbell [17, 24] demonstrated the thermal entrainment process and argued in more detail for the plume head explanation of flood basalts. In particular Griffiths and Campbell argued that plume heads could reach much larger diametres, 800–1200 km, than had previously been estimated, if they rise from the bottom of the mantle, and also that they would

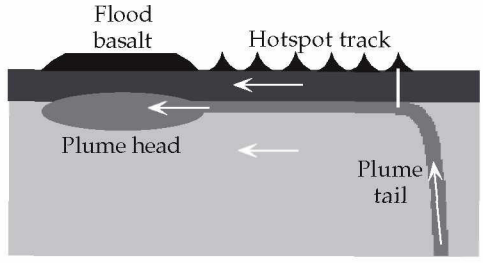

Figure 11.13. Sketch of the way a new plume with a head-and-tail structure can account for the relationship observed between some flood basalts and hotspot tracks, in which the hotspot track emerges from a flood basalt province and connects it to a currently active volcanic hotspot. It is assumed in the sketch that the plate and subjacent mantle are moving to the left relative to the plume source.

approximately double in horizontal diameter as they flattened and spread below the lithosphere (Figures 11.6, 11.10). This is in good agreement with the observed total extents of flood basalt provinces, the Karoo flood basalts being scattered over a region about 2500 km in diameter. Campbell and Griffiths argued that important aspects of the petrology and geochemistry of flood basalts could be explained by the model, in particular the concentration near the centres of provinces of picrites, which are products of higher degrees of melting than basalts. They argued that this can be explained by the temperature distribution of a plume head, which is hottest at the central conduit and cooler to the sides (Figure 11.6).

Though this model of flood basalt formation has attracted wide interest, it has not yet been fully explored quantitatively. The principal outstanding question is whether it can account quantitatively for the observed volumes of flood basalts in cases where there appears to have been little or no rifting. The perceived problem has been that normal mantle compositions do not begin to melt until they have risen to depths less than about 120 km even if they are 200 °C hotter than normal [29, 30]. Since continental lithosphere is commonly at least this thick, we would not expect plumes to melt at all under continents.

However plumes are known not to have normal mantle composition. It is widely recognised by geochemists on the basis of trace element contents that they have a larger complement of basaltic composition than normal mantle. This component of their composition is hypothesised to come from previously subducted oceanic crust that is entrained in plumes near the base of the mantle (Chapter 13; [21]). Such a composition would substantially lower the solidus temperature and enhance melt production. Some preliminary models [31] and continuing work indicate that melt volumes of the order of 1 million cubic kilometres can be produced from such a plume head. Examples of calculations of melt volume from a simplified plume head model with an enhanced basaltic component are shown in Figure 11.14. These show that it is plausible that several million cubic kilometres of magma could be erupted within about 1 Ma.

Other factors being evaluated for their influence on plume head melting are higher plume temperatures [32], the effect of mantle viscosity structure on the height to which plumes can penetrate, noted in Section 11.4.4 (Figure 11.10), or that plumes may be more effective at thinning the lithosphere and penetrating to shallow depths than has been recognised. The indications at this stage are that a satisfactory quantitative account of flood basalts will

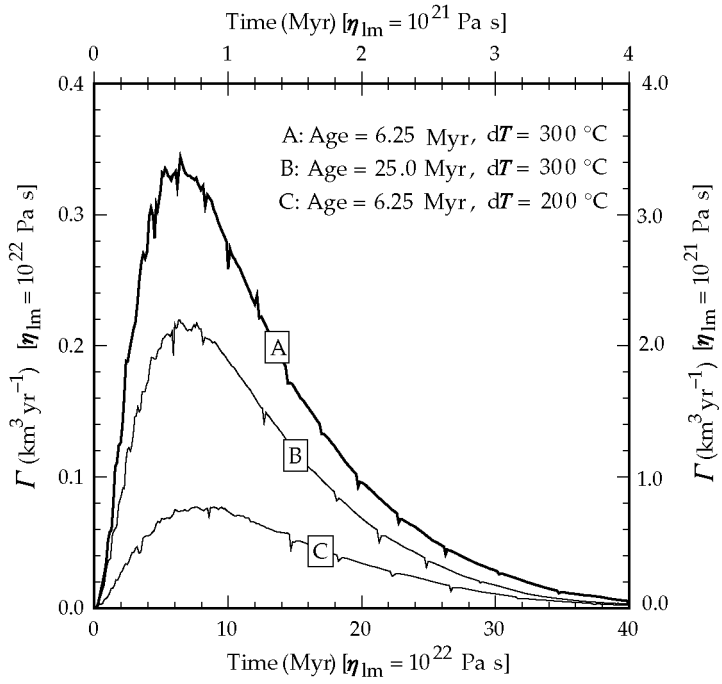

Figure 11.14. Calculated rates of magma generation, Γ, from a simplified numerical model of a plume head that includes 15% additional basaltic component. The curves assume different initial plume temperature excesses, dT, and different ages (and thus thicknesses) of lithosphere. The plume head was modelled as a sphere with initially uniform temperature. The left and bottom scales assume a mantle viscosity of 10^{22} Pa s, the right and top scales are for 10^{21} Pa s. From Cordery *et al.* [31]. Copyright by the American Geophysical Union.

emerge from the plume head model, but this has not yet been attained.

11.6 Some alternative theories

11.6.1 Rifting model of flood basalts

White and McKenzie [30] proposed a theory for the formation of very thick sequences of volcanic flows found along some continental margins and of flood basalt eruptions. The theory can usefully be separated into three parts. The first part is that the marginal volcanic provinces are produced when rifting occurs over a region of mantle that is hotter than normal because it is derived from a plume. This seems to give a very viable account of such provinces. The second part is that all flood basalts can be explained by this

mechanism. The third part is that the plume material is derived mainly from a plume tail, since they assumed that plumes are part of an upper mantle convection system and that plumes therefore derive from no deeper than 670 km. In this case the plume heads would have diameters of no more than about 300 km and volumes less than about 5% of a plume head from the bottom of the mantle [24].

The second part of White and McKenzie's model encounters the difficulty that a number of flood basalt provinces are said, on the basis of field evidence, to have erupted mainly before substantial rifting occurred (e.g. Deccan Traps) or in the absence of any substantial rifting (e.g. Siberian Traps, Columbia River Basalts) [33]. It also fails to explain the very short time scale of flood basalt eruptions, less than 1 Ma in the best-constrained cases. The third part of their model implies that a sufficient volume of warm mantle would take about 50 Ma to accumulate, but at the time the Deccan Traps erupted, India was moving north at about 180 mm/yr (180 km/Ma) so it would have traversed the extent of the flood basalts in only about 10 Ma. It is difficult to see how sufficient warm mantle could accumulate from a plume tail under such a fast-moving plate.

These difficulties are avoided by the plume head model of flood basalts, since the flow rate of the plume head is much greater than the tail and much of the melting is inferred to occur from beneath the intact lithosphere upon arrival of the plume head. It is true that the volumes of the eruptions have yet to be fully explained quantitatively, but current indications are that this is not a fundamental difficulty.

11.6.2 Mantle wetspots

Green [34] has argued that volcanic hotspots can be explained by mantle 'wetspots'. From a petrological point of view, this idea has some merits, since a small amount of water (less than 0.1%) can substantially reduce the solidus temperature, at which melting first occurs. It is also true that hydrated forms of minerals are generally less dense than their dry counterparts, which could provide the buoyancy required to explain hotspot swells. The effect on density needs to be better quantified, and it would need to be shown that observed water contents of hotspot volcanics are consistent with the amounts required to explain the buoyancy. It needs also to be shown that sufficient melt can be produced to explain the observed volcanism, since although water reduces the solidus temperature,

substantial degrees of melting still do not occur until the dry solidus temperature is approached.

However, a remaining difficulty would still be to explain the duration of long-lived volcanic centres like Hawaii. While a hydrated portion of the mantle, perhaps old subducted oceanic crust, might produce a burst of volcanism, there is no explanation offered for how the source might persist for 100 Ma or more. It is useful to estimate the volume of mantle required to supply the Hawaiian plume for 100 Ma. The total volume erupted into the Hawaiian and Emperor seamounts over 90 Ma is about $10^6\,\mathrm{km}^3$. If we assume that there was about 5% melting of the source, this requires a source volume of $2 \times 10^7\,\mathrm{km}^3$, equivalent to a sphere of diameter 340 km. If such a large and buoyant region existed as a unit in the mantle, it would rise and produce a burst of volcanism. To explain the Hawaiian volcanic chain the hydrated mantle material needs to be supplied at a small and steady rate.

The advantage of the thermal plume hypothesis is that a renewal mechanism is straightforwardly provided if the plume originates from a thermal boundary layer. It may be that the effects of water on melting and on plume buoyancy are significant, but it is far from clear that water alone could provide a sufficient explanation of the observations, while heat alone, or heat plus water, provides a straightforward and quantitatively successful account of the dynamical requirements of a theory of plumes.

11.6.3 Melt residue buoyancy under hotspot swells

J. P. Morgan and others [19] have proposed that the buoyancy supporting hotspot swells is due significantly also to the compositional buoyancy of the residue remaining after the hotspot magma has erupted. The residue will be less dense because iron partitions preferentially into the melt phase. However, the estimates made in Sections 11.2 and 11.3 indicate that the amount of melt produced is less than 1% of the volume of the plume material, in which case this will be a minor effect. Morgan and others estimate the density change of the residue as a function of mean melt fraction, f, from the formula

$$\Delta\rho = \rho_{\mathrm{m}}\beta f$$

where $\beta = 0.06$ is an empirically evaluated constant. This implies that the annual volume of mantle that arrives through the plume should expand by the same fraction, βf, and this expansion is what is manifest as the plume swell. We can therefore estimate the annual

contribution to the swell volume from the effect of residue buoyancy as

$$\Phi_{sr} = \Phi_p \beta f$$

Using the values $\Phi_p = 7.5\,km^3/a$ and $f = 0.01$, used earlier for Hawaii, this gives $\Phi_{sr} = 0.0045\,km^3/a$, which is only about 5% of the observed rate of swell formation of $0.1\,km^3/a$. While the residue buoyancy may be more significant locally under the volcanic chain, it seems that the direct buoyancy of the plume material is still required to account for most of the Hawaiian swell. This implies in turn that the estimates of buoyancy and heat flow rate given in Section 11.2 are reasonable.

11.7 Inevitability of mantle plumes

The earth is believed to have been strongly heated during the late stages of its formation. The heat comes from the release of gravitational energy of material falling onto the growing earth. The earth is believed to have formed from a disk of particles orbiting the sun and left over from the sun's formation. Models of the process of accumulation of material into larger bodies indicate that many bodies would grow simultaneously, but that there would be a wide distribution of sizes, with only a few large bodies and greater numbers of smaller bodies. In this situation the final stages of accumulation would involve the collision of very large bodies. A plausible and currently popular theory for the formation of the moon proposes that the moon was formed from the debris of a collision of a Mars-sized body with the earth. A collision of this magnitude would probably have melted much of the earth, and vaporised some of it. Accounts of these ideas can be found in [35, 36, 37].

Suppose that the earth was heated in this way, and that it quickly homogenised thermally, as a substantially liquid body would do. The temperature would not be uniform, but would follow an adiabatic profile with depth, due to the effect of pressure, as discussed in Chapter 7. The earth's temperature as a function of depth would therefore look like curve (a) sketched in Figure 11.15.

The earth would then lose heat through its surface. This would form an outer thermal boundary layer (a precursor to the lithosphere) and, with the mantle being very hot and possibly partially molten, rapid mantle convection could be expected. In this way the mantle would be cooled. Suppose, for the simplicity of this argument, that the entire mantle convected and cooled in this way.

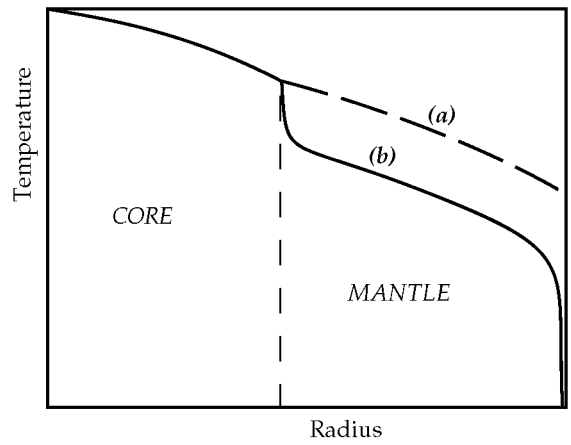

Figure 11.15. Sketch of the form of the temperature profile within the earth (a) soon after formation, and (b) later, after the mantle has cooled by heat loss to the surface. The core can only begin to lose heat after the mantle has become cooler than the core. Thereafter the heat conducting from the core into the base of the mantle forms a thermal boundary layer that can generate buoyant upwellings.

After some time, the temperature profile would have looked like curve (b) of Figure 11.15.

Initially, the core would not have been able to lose heat, because we assumed that the mantle and core had the same temperature at their interface. However, as the mantle cooled, heat would begin to conduct out of the core into the base of the mantle, and cooling of the core would commence. This heat from the core would form a thermal boundary layer at the base of the mantle, depicted in curve (b) of Figure 11.15. If the mantle viscosity were sufficiently low and the heat flow from the core sufficiently high, both of which are highly likely, this thermal boundary layer would become unstable and buoyant upwellings would rise from it. These upwellings would have a lower viscosity than the mantle they were rising through, so they would develop a head-and-tail structure, as discussed in Section 11.4.

Thus we have a general argument for the existence of thermal plumes in the mantle. The assumptions are that the core and mantle started with similar temperatures at their interface, that the mantle has been cooling, and that the conditions are such that the relevant Rayleigh number is greater than its critical value for instability and convection to occur. If the earth, now or in the past, functioned as more than two independent layers, then the argument generalises very simply: the layers would cool from the outside inwards, and

plumes would be generated in each layer by heat conducting from the next deeper layer.

11.8 The plume mode of mantle convection

We have seen that the existence of volcanic island and seamount chains terminating in isolated active volcanic hotspots, such as Hawaii, and surrounded by broad topographic swells imply the existence of narrow, long-lived columns of buoyant, rising mantle material. Morgan called these mantle plumes. The buoyancy and excess melting can be explained if the plumes are 200–300 °C hotter than normal mantle, and their longevity is plausible if they derive from a hot thermal boundary layer. Their higher temperature implies that plumes would have lower viscosity than normal mantle. Fluid dynamics experiments show that the preferred form of low-viscosity buoyant upwellings is columnar, and that new plumes would start with a large, spherical head. Plume heads are calculated to reach diameters of about 1000 km near the top of the mantle, and they provide a plausible explanation for flood basalt eruptions. The association of plume heads with their following plume tails provides an explanation for hotspot tracks that emerge from flood basalt provinces.

Plumes and the flow they drive in surrounding mantle comprise a distinct mode of mantle convection, driven by a hot, lower thermal boundary layer. They therefore complement the plate mode driven by the cool, top thermal boundary layer. As with the plate mode, there will be a passive downward return flow driven by plumes that balances the upflow in plumes. The fact that hotspot locations do not correlate strongly with the current configuration of plates (Figure 11.1; [38]) indicates that the plume and plate modes are not strongly coupled. The implication is that plumes rise through the plate-scale flow without substantially disrupting it. Experiments have shown that plume tails can rise through a horizontal background flow, bending away from the vertical but retaining their narrow tubular form [39, 40, 41]. However, there is a correlation between plume locations, broad geoid highs and slower seismic wavespeeds in the deep mantle [38, 42], indicating that plumes form preferentially away from deeply subducted lithosphere.

Plumes may have been significant tectonic agents through much of earth history. They may trigger ridge jumps or occasional larger-scale rifting events [5, 43]. Plume heads have been proposed as the direct source of Archean greenstone belts and the indirect cause, through their heat, of associated granitic terrains from sec-

ondary crustal melting [44]. They may have been a significant source of continental crust, directly from continental flood basalts and through the accretion as exotic terrains of oceanic flood basalts [14, 45]. They may be the source of many dike swarms, and as a source of heat they may have been involved in some regional 'anorogenic' crustal heating and melting events and in the reworking and mineralising of a significant proportion of the continental crust [14]. The term 'plume tectonics' has been used to encapsulate their possibly substantial tectonic role [14].

A fundamental aspect of mantle convection is that the thermal boundary layers are distinct agents, as I stressed in Chapter 8. It is therefore incorrect to regard plumes and plume tectonics as a possible substitute for plate tectonics, as has been speculated not infrequently for the early earth and for Venus. Currently in the earth, plate tectonics cools the mantle. If plate tectonics did not operate, then the top boundary layer would have to operate in another way in order to remove heat from the mantle. The role of plumes is to transfer heat from the layer below (the core) into the convecting mantle. Any surface heat flow or tectonic effect from plumes is incidental, and adds to whatever tectonics are driven by the top boundary layer. This will be discussed in more detail in Chapter 14.

A further implication of this last point is that the level of activity of plumes depends on the strength of the hot thermal boundary layer at the base of the mantle. This may have varied with time, though calculations suggest that it may have been rather constant (Chapter 14). It follows also that the two thermal boundary layers need to be prescribed separately in numerical models of mantle convection. In other words, it is sensible to define separate Rayleigh numbers for each thermal boundary layer, and hence for each mode of mantle convection.

11.9 References

1. T. S. Crough and D. M. Jurdy, Subducted lithosphere, hotspots and the geoid, *Earth Planet. Sci. Lett.* **48**, 15–22, 1980.
2. R. A. Duncan and M. A. Richards, Hotspots, mantle plumes, flood basalts, and true polar wander, *Rev. Geophys.* **29**, 31–50, 1991.
3. J. T. Wilson, A possible origin of the Hawaiian islands, *Can. J. Phys.* **41**, 863–70, 1963.
4. W. J. Morgan, Convection plumes in the lower mantle, *Nature* **230**, 42–3, 1971.
5. W. J. Morgan, Plate motions and deep mantle convection, *Mem. Geol. Soc. Am.* **132**, 7–22, 1972.

6. W. J. Morgan, Hotspot tracks and the opening of the Atlantic and Indian Oceans, in: *The Sea*, C. Emiliani, ed., Wiley, New York, 443–87, 1981.
7. K. C. Burke and J. T. Wilson, Hot spots on the earth's surface, *Sci. Am.* **235**, 46–57, 1976.
8. M. A. Richards, B. H. Hager and N. H. Sleep, Dynamically supported geoid highs over hotspots: observation and theory, *J. Geophys. Res.* **93**, 7690–708, 1988.
9. A. B. Watts and U. S. ten Brink, Crustal structure, flexure and subsidence history of the Hawaiian Islands, *J. Geophys. Res.* **94**, 10 473–500, 1989.
10. D. L. Turcotte and G. Schubert, *Geodynamics: Applications of Continuum Physics to Geological Problems*, 450 pp., Wiley, New York, 1982.
11. G. F. Davies, Ocean bathymetry and mantle convection, 1. Large-scale flow and hotspots, *J. Geophys. Res.* **93**, 10 467–80, 1988.
12. N. H. Sleep, Hotspots and mantle plumes: Some phenomenology, *J. Geophys. Res.* **95**, 6715–36, 1990.
13. F. D. Stacey, *Physics of the Earth*, 513 pp., Brookfield Press, Brisbane, 1992.
14. R. I. Hill, I. H. Campbell, G. F. Davies and R. W. Griffiths, Mantle plumes and continental tectonics, *Science* **256**, 186–93, 1992.
15. F. D. Stacey and D. E. Loper, Thermal histories of the core and mantle, *Phys. Earth Planet. Inter.* **36,** 99–115, 1984.
16. R. P. Von Herzen, M. J. Cordery, R. S. Detrick and C. Fang, Heat flow and thermal origin of hotspot swells: the Hawaiian swell revisited, *J. Geophys. Res.* **94**, 13 783–99, 1989.
17. I. H. Campbell and R. W. Griffiths, Implications of mantle plume structure for the evolution of flood basalts, *Earth Planet. Sci. Lett.* **99**, 79–83, 1990.
18. D. A. Clague and G. B. Dalrymple, Tectonics, geochronology and origin of the Hawaiian-Emperor volcanic chain, in: *The Eastern Pacific Ocean and Hawaii*, E. L. Winterer, D. M. Hussong and R. W. Decker, eds., Geological Society of America, Boulder, CO, 188–217, 1989.
19. J. P. Morgan, W. J. Morgan and E. Price, Hotspot melting generates both hotspot swell volcanism and a hotspot swell?, *J. Geophys. Res.* **100**, 8045–62, 1995.
20. P. Wessel, A re-examination of the flexural deformation beneath the Hawaiian islands, *J. Geophys. Res.* **98**, 12 177–90, 1993.
21. A. W. Hofmann and W. M. White, Mantle plumes from ancient oceanic crust, *Earth Planet. Sci. Lett.* **57**, 421–36, 1982.
22. J. A. Whitehead and D. S. Luther, Dynamics of laboratory diapir and plume models, *J. Geophys. Res.* **80**, 705–17, 1975.
23. M. A. Richards, R. A. Duncan and V. E. Courtillot, Flood basalts and hot-spot tracks: plume heads and tails, *Science* **246**, 103–7, 1989.

24. R. W. Griffiths and I. H. Campbell, Stirring and structure in mantle plumes, *Earth Planet. Sci. Lett.* **99**, 66–78, 1990.
25. I. H. Campbell and R. W. Griffiths, The evolution of the mantle's chemical structure, *Lithos* **30**, 389–99, 1993.
26. M. A. Richards and R. W. Griffiths, Deflection of plumes by mantle shear flow: experimental results and a simple theory, *Geophys. J.* **94**, 367–76, 1988.
27. G. F. Davies, Penetration of plates and plumes through the mantle transition zone, *Earth Planet. Sci. Lett.* **133**, 507–16, 1995.
28. M. F. Coffin and O. Eldholm, Large igneous provinces: crustal structure, dimensions and external consequences, *Rev. Geophys.* **32**, 1–36, 1994.
29. D. P. McKenzie and M. J. Bickle, The volume and composition of melt generated by extension of the lithosphere, *J. Petrol.* **29**, 625–79, 1988.
30. R. White and D. McKenzie, Magmatism at rift zones: the generation of volcanic continental margins and flood basalts, *J. Geophys. Res.* **94**, 7685–730, 1989.
31. M. J. Cordery, G. F. Davies and I. H. Campbell, Genesis of flood basalts from eclogite-bearing mantle plumes, *J. Geophys. Res.* **102**, 20 179–97, 1997.
32. C. Farnetani and M. A. Richards, Numerical investigations of the mantle plume initiation model for flood basalt events., *J. Geophys. Res.* **99**, 13 813–33, 1994.
33. P. R. Hooper, The timing of crustal extension and the eruption of continental flood basalts, *Nature* **345**, 246–9, 1990.
34. D. H. Green and T. J. Falloon, Pyrolite: A Ringwood concept and its current expression, in: *The Earth's Mantle: Composition, Structure and Evolution*, I. N. S. Jackson, ed., Cambridge University Press, Cambridge, 311–78, 1998.
35. G. W. Wetherill, Occurrence of giant impacts during the growth of the terrestrial planets, *Science* **228**, 877–9, 1985.
36. G. W. Wetherill, Formation of the terrestrial planets, *Annu. Rev. Astron. Astrophys.* **18**, 77–113, 1980.
37. H. E. Newsom and J. H. Jones, *Origin of the Earth*, 378, Oxford University Press, New York, 1990.
38. M. Stefanick and D. M. Jurdy, The distribution of hot spots, *J. Geophys. Res.* **89**, 9919–25, 1984.
39. M. A. Richards and R. W. Griffiths, Thermal entrainment by deflected mantle plumes, *Nature* **342**, 900–2, 1989.
40. R. W. Griffiths and I. H. Campbell, On the dynamics of long-lived plume conduits in the convecting mantle, *Earth Planet. Sci. Lett.* **103**, 214–27, 1991.
41. R. W. Griffiths and M. A. Richards, The adjustment of mantle plumes to changes in plate motion, *Geophys. Res. Lett.* **16**, 437–40, 1989.
42. M. A. Richards and D. C. Engebretson, Large-scale mantle convection and the history of subduction, *Nature* **355**, 437–40, 1992.

43. R. I. Hill, Starting plumes and continental breakup, *Earth Planet. Sci. Lett.* **104**, 398–416, 1991.
44. I. H. Campbell and R. I. Hill, A two-stage model for the formation of the granite-greenstone terrains of the Kalgoorlie-Norseman area, Western Australia, *Earth Planet. Sci. Lett.* **90**, 11–25, 1988.
45. M. A. Richards, D. L. Jones, R. A. Duncan and D. J. DePaolo, A mantle plume initiation model for the Wrangellia flood basalt and other oceanic plateaus, *Science* **254**, 263–7, 1991.